

1
2
3
4
5
6
7
8
9
10
11
12
13
14
15
16
17
18
19
20
21
22
23
24
25
26
27
28
29
30
31
32
33
34
35
36
37
38
39
40

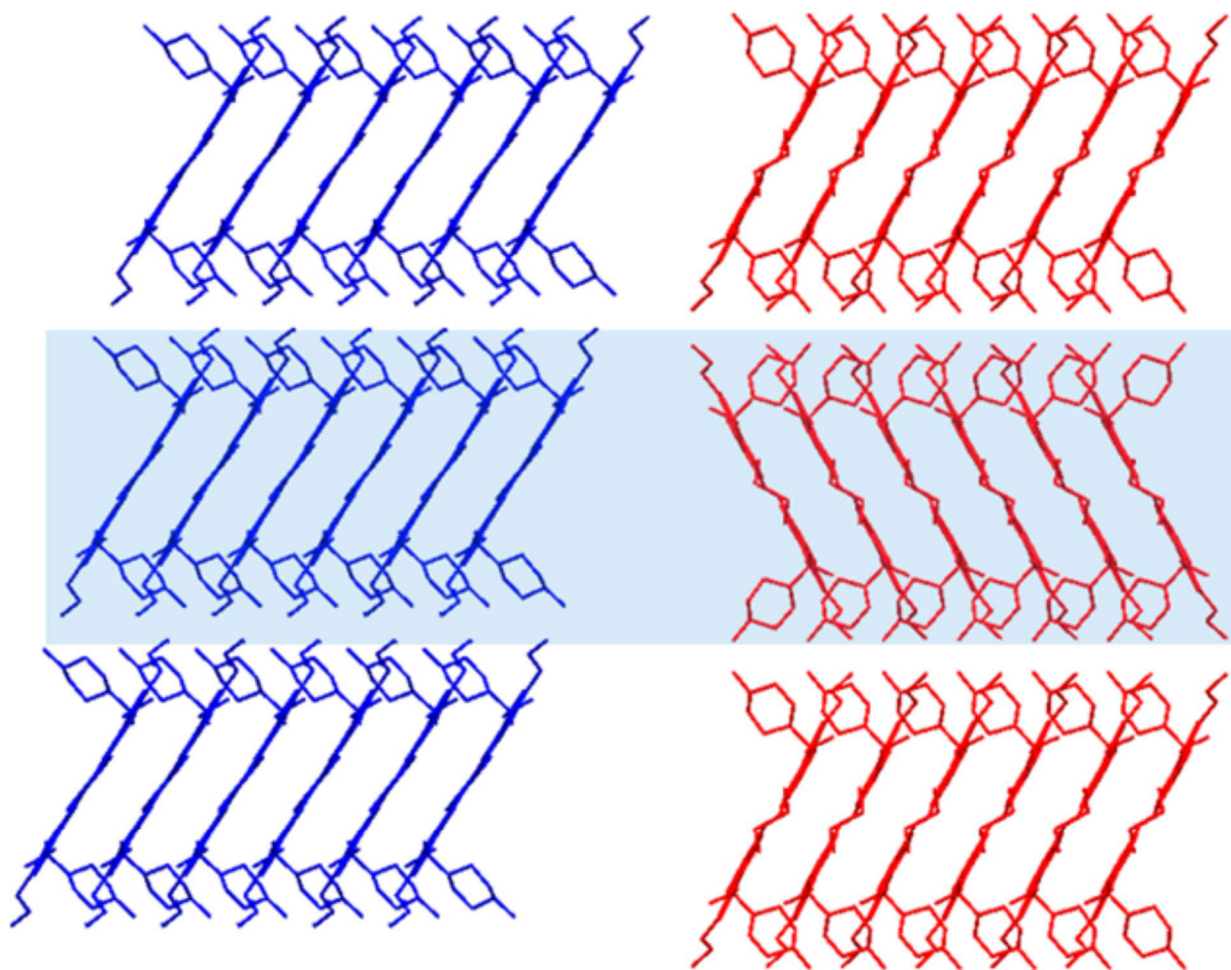
Polymorphism of Sildenafil: A New Metastable Desolvate

Rafael Barbas,[†] Mercè Font-Bardia,[§] and Rafel Prohens^{*,†}

[†]Unitat de Polimorfisme i Calorimetria, Centres Científics i Tecnològics and [§]Unitat de Difracció de Raigs X, Centres Científics i Tecnològics, Universitat de Barcelona, Baldri Reixac 10, 08028 Barcelona, Spain

41 **ABSTRACT:**

42
43 A new anhydrous polymorph of the free base of sildenafil and two solvates (acetonitrile and
44 propanenitrile) have been discovered and fully characterized. The new polymorph can be considered a
45 desolvate of the acetonitrile solvate and is related to the most stable form I by morphotropism. The new
46 polymorph can only be obtained by desolvation of the acetonitrile solvate. Thus, this study is a new
47 example of the importance of this multicomponent family of solid forms in the discovery of new
48 polymorphs of active pharmaceutical ingredients.
49



50 **Form I**

51 **Form II**

52
53
54

55 1. INTRODUCTION

56

57 Active pharmaceutical ingredients (APIs) can exist in addition to polymorphs as solvates, a phenomenon
58 known as pseudopolymorphism.¹ Since APIs are small molecular weight compounds, they tend to form
59 solvates and hydrates where solvent molecules are an integral part of the solid form structure. In
60 particular, water molecules can occupy isolated sites (stoichiometric hydrates) or channels
61 (stoichiometric and nonstoichiometric hydrates).² Frequently, the removal of water molecules produces
62 the collapse of the crystal network with the result of an amorphous³ form or an anhydrous
63 polymorph.^{4,5}

64 Although it has been suggested that 33% of organic compounds can form hydrates but only 10% of them
65 can form solvates,⁶ the formation of solvates can have important consequences during the development
66 of an API because they can affect their physicochemical properties such as stability or solubility in
67 relation to the anhydrous form.^{7,8} The Cambridge Structural Database (CSD) has been searched in
68 order to study the frequency of solvate formation, and more than 300 different solvent molecules were
69 identified to form a solvate.⁹ Moreover, hydrate formation in organic compounds and the important
70 factors determining the high frequency of hydrates have been studied by analyzing the CSD,¹⁰ and
71 statistical models for the prediction of hydrate and solvate formation have been developed.¹¹

72 API solvates are generally prepared by recrystallization, but hydrates may also appear during
73 formulation of a drug while being exposed to air. But while pharmaceutical hydrates are viable forms for
74 drug products because there is no safety concern about water as a crystal adduct, solvates are rarely
75 formulated because of safety concerns due to solvent toxicity.^{12,13} However, the phenomenon of
76 pseudopolymorphism can have a significant impact in the development of a pharmaceutical drug since
77 the pharmaceutical drugs are usually in contact with organic solvent during the purification and
78 processing stages.¹⁴ Particularly relevant is the case of sulfathiazole,¹⁵ which forms over 100 solvates.
79 Usually solvate structures collapse immediately after the removal of the solvent; however, in some cases
80 isomorphic desolvates are formed when the solvent molecules are removed without the collapse of the
81 crystal network and retain most of the packing issues of the parent solvate.¹⁶ Thus, isomorphic
82 desolvates can be regarded as different polymorphs but constitute a specific category of solid forms
83 since they can only be formed by desolvation and stabilized in the absence of solvent molecules.¹⁷ The
84 presence of voids in the desolvate structure is related to its usual tendency to be hygroscopic^{18,19} and to
85 a lower stability based on a reduced packing efficiency.²⁰ In some cases, the desolvation produces very
86 small crystallites that although crystalline at a local level give poorly defined powder X-ray diffraction
87 (PXRD) patterns, which hinder their characterization.²¹ Although hydrates and solvates constitute a
88 topic of continuous research interest in the pharmaceutical industry, isomorphic desolvates have been
89 scarcely explored in the crystal engineering field to date.²² Thus, in this paper we report a new
90 isomorphic desolvate of the free base of sildenafil which is morphotropically related to the known
91 anhydrous form I. The study has been completed with the full characterization of new acetonitrile and

92 propanenitrile solvates of sildenafil, which are key to understanding the role of the solvent in the
93 discovery of the new polymorph of sildenafil.

94

95

96

97 **2. MATERIALS AND METHODS**

98

99 **2.1. Materials.** Sildenafil used in this study was of reagent grade and used as received from Polpharma
100 (form I). Anhydrous form II has been obtained by slurring sildenafil (form I) in ACN followed by fast
101 drying under a vacuum (30 min) at 25 °C. ACN solvate (form ACNI) has been obtained by slow
102 crystallization in ACN after 37 days at 25 °C. ACN solvate (form ACNII) has been obtained after
103 keeping sildenafil (form I) in ACN atmosphere for 2 weeks. Propanenitrile solvate has been obtained by
104 slow crystallization in propanenitrile after 1 day at 25 °C.

105 **2.2. Methods.** 2.2.1. X-ray Crystallographic Analysis. Single crystal X-ray diffraction intensity data of
106 sildenafil form I and acetonitrile solvate form ACNI were collected using a D8 Venture system equipped
107 with a multilayer monochromator and a Mo microfocus ($\lambda = 0.71073 \text{ \AA}$). Frames were integrated with
108 the Bruker SAINT software package using a SAINT algorithm. Data were corrected for absorption
109 effects using the multiscan method (SADABS).²³ The structure was solved and refined using the Bruker
110 SHELXTL Software Package, a computer program for automatic solution of crystal structures and
111 refined by full-matrix least-squares method with ShelXle Version 4.8.0, a Qt graphical user interface for
112 SHELXL computer program.²⁴

113 Powder X-ray diffraction pattern of form II was obtained on a PANalytical X'Pert PRO MPD
114 diffractometer in transmission configuration using Cu $K\alpha_{1+2}$ radiation ($\lambda = 1.5406 \text{ \AA}$) with a focusing
115 elliptic mirror and a PIXcel detector working at a maximum detector's active length of 3.347° .
116 Configuration of convergent beam with a focalizing mirror and a transmission geometry with flat
117 sample sandwiched between low absorbing films measuring from 2 to 80° in 2θ , with a step size of
118 0.013° and a total measuring time of 2 h. The powder diffractogram data were perfectly indexed to a
119 orthorhombic cell of about 4954 \AA^3 by means of Dicvol04,²⁵ and the space group perfectly was
120 determined to be Pccn from the systematic absences. With one independent molecule of sildenafil in the
121 asymmetric unit, $Z = 8$, the crystal structure was determined by direct space methodologies starting from
122 a molecular model optimized with the commercial software SPARTAN²⁶ by means of the program
123 FOX²⁷ with the parallel tempering algorithm. Some constraints were introduced to FOX, considering
124 aromatic rings as rigid groups. Several trials of 20 million runs were performed. The refinement of the
125 structure has been performed by the Rietveld method using FullProf;²⁸ Figure 2 depicts the final
126 Rietveld plot. The crystal structure of anhydrous form I has been solved at room temperature from single
127 crystal X-ray diffraction (SXRD) in order to compare with form II since the structures deposited at the
128 CSD²⁹ have been solved at different temperatures. A summary of crystal data and relevant refinement
129 parameters are given in Table 1.

130 2.2.2. Differential Scanning Calorimetry (DSC). Differential scanning calorimetry analysis were carried
131 out by means of a Mettler-Toledo DSC-822e calorimeter. Experimental conditions: aluminum crucibles
132 of $40 \mu\text{L}$ volume, atmosphere of dry nitrogen with 50 mL/min flow rate, heating rate of $10 \text{ }^\circ\text{C/min}$. The
133 calorimeter was calibrated with indium of 99.99% purity (m.p.: $156.4 \text{ }^\circ\text{C}$, ΔH : 28.55 J/g).

134 2.2.3. Thermogravimetric Analysis (TGA). Thermogravimetric analyses were performed on a Mettler-
135 Toledo TGA-851e thermobalance. Experimental conditions: alumina crucibles of $70 \mu\text{L}$ volume,
136 atmosphere of dry nitrogen with 50 mL/min flow rate, and heating rate of $10 \text{ }^\circ\text{C/min}$.

137 2.2.4. Dynamic Vapor Sorption (DVS). The water sorption and desorption processes were measured on
138 a DVS-1000 instrument from Surface Measurement Systems. The samples were mounted on a balance
139 and studied over a humidity range from 0% to 90% RH, and then decreased to 0% RH at 25 and $40 \text{ }^\circ\text{C}$
140 using a three-cycle method. The equilibrium condition for each step was set to a mass constancy of
141 $\pm 0.001\%$ over 60 min and a maximum time limit of 1440 min for each step.

142

143 3. RESULTS AND DISCUSSION

144

145 Sildenafil, the ingredient of Viagra, is the first oral drug used for the medical treatment of erectile
146 dysfunction and has been recently used for the treatment of pulmonary hypertension^{30,31} but due to its
147 low water solubility it is generally formulated as sildenafil citrate.³² The crystal structures of sildenafil
148 base, sildenafil citrate monohydrate, and sildenafil saccharinate have been reported elsewhere.²⁹ With
149 the aim to study the solid state of this API, we conducted an extensive polymorph screening by using a
150 broad set of thermodynamic and kinetic experimental conditions from a variety of 54 solvents,³³ which
151 produced 98 individual crystalline solids. Six new solvates (toluene, anisole, acetonitrile, propanenitrile,
152 dioxane, and chloroform) and a new polymorph of sildenafil have been discovered, and their crystal
153 structures were solved. The density functional theory (DFT) analysis of toluene, anisole, dioxane, and
154 chloroform solvates is the subject of another research paper, in which the formation of an apparently
155 innocent intramolecular H-bond has a remarkable influence on the solid state architecture of the
156 sildenafil solvates.³⁴

157 During the polymorph screening with 53 out of 54 organic solvents only the known form I or new
158 solvates (as mentioned before) were obtained except when acetonitrile was used. In particular,
159 crystallizing or slurrying in this solvent produced three new solid forms depending on whether the solid
160 obtained was extensively dried or not. When the solid obtained by slurrying sildenafil in acetonitrile was
161 dried under a vacuum, an anhydrous new form (form II) was obtained, but if the solid was only filtered
162 and directly analyzed without further drying, a new solvate (form ACNII) was produced with 2:1
163 sildenafil/acetonitrile stoichiometry (deduced from TGA, Figure S10). Moreover, needles of a different
164 acetonitrile solvate with 1:1 sildenafil/acetonitrile stoichiometry were obtained (solvate form ACNI) by
165 slow evaporation of an acetonitrile solution of sildenafil at room temperature, and its crystal structure
166 was solved by SXRD analysis. The PXRD diffractogram of solvate form ACNII was indexed (Figure
167 S13) at room temperature, and its stoichiometry was deduced from TGA (Figure S10). The two solvates
168 show a very similar PXRD diagram and cell parameters, which suggests that both solvates can be
169 isostructural, Figure 3. See Supporting Information for further detail.

170 The DSC of sildenafil form II shows two overlapped endothermic/exothermic phenomena prior to the
171 melting of form I (Figure 4), while modulated DSC (Figure S8, Supporting Information) shows in the
172 reversing signal an increase of heat capacity without melting followed by an exothermic broad peak in
173 the nonreversing signal, suggesting that form II transforms into form I upon heating through a two-step
174 process involving a glass-like solid. On the other hand, desolvation of solvate form ACNII by air drying
175 at room temperature produced the new anhydrous form II, while DSC of solvate form ACNII showed a
176 melting point, which is 5 °C lower than form I, probably due to lower crystallinity of the sample after
177 desolvation and recrystallization (Figures 4, S9 and S10). The crystal structure of the new anhydrous
178 form II was solved by means of direct space strategies from PXRD data, and the analysis of the crystal
179 structures reveals that anhydrous form II is an isomorphic desolvate of the new acetonitrile solvate form

180 ACNI. Figure 5 shows that the only significant difference between both forms is the more opened
181 conformation of the propyl groups in the desolvate which cannot completely fill the voids left by the
182 removed solvent. The fact that anhydrous form II has only been detected in 1 out of 54 solvents can
183 explain why new anhydrous form II has not been previously reported in the literature and points out an
184 important conclusion of this work as it will be discussed later.

185 The crystal structures of the two anhydrous forms at room temperature have been compared, and a
186 careful analysis of the packing reveals that the asymmetric unit independent molecules of both forms
187 establish the same strong intramolecular hydrogen bond between the ethoxy oxygen and the pyrimidine
188 nitrogen. Thus, the observed differences can be considered as conformational adjustments of the same
189 gasphase conformer, according to the cutoff value proposed by Cruz-Cabeza and Bernstein in their
190 analysis of conformational polymorphism³⁵ since the root-mean-square distance (RMSD) value
191 computed using Mercury is less than 0.375 Å. Among the observable conformational adjustments, the
192 most relevant one involves the propyl groups, Figure 6.

193 This can be better visualized through the fingerprint plots^{36,37} from Hirshfeld surfaces.³⁸ Although the
194 essential features of the intermolecular atom–atom contacts are very similar, in form II the H···H
195 contacts (highlighted with a black circle in Figure 7) are much shorter than in form I as a consequence of
196 the necessary folding of the propyl groups to maintain free the cavity previously occupied by the
197 acetonitrile molecules in the solvate. In acetonitrile solvate ACNI the short H···H contacts were already
198 present, and while anhydrous form I has a more extended configuration with less short H···H contacts
199 the desolvate form II keeps much of the parent structure of the ACNI solvate, which explains why the
200 short H···H contacts are also present in form II (see Tables 1 and 2 of Supporting Information). These
201 interatomic contacts are presumably repulsive according to the accepted van der Waals diameter of the
202 hydrogen atom (1.1–1.2 Å). However, only a small number of organic crystal structures have been
203 reported with H···H interatomic distances lower than 2.2 Å,³⁹ which are associated with repulsive
204 forces to preserve the internal equilibrium in the crystal structure,⁴⁰ as appears to be the case of
205 anhydrous form II and solvate form ACNI. See Supporting Information for further detail.

206 The most important consequence of anhydrous form II being an isomorphic desolvate of acetonitrile
207 solvate is that there are bigger finite voids (rather than interconnected channels) than in form I. These
208 have been calculated using the contact surface model using Mercury with a probe of 0.88 Å radius and
209 shown in Figure 8. Since crystal structures of anhydrous form I and solvate ACNI have been solved at
210 room temperature, there is disorder on the propyl groups (not present at 100 K, data not shown), which
211 can be explained based on the fact that propyl groups do not establish strong intermolecular interactions
212 with the surrounding atoms. This disorder is also probably present in anhydrous form II because the
213 voids are bigger; however since the structure has been solved by direct space methods from PXRD, the
214 disorder cannot be directly measured.

215 On the other hand, the intermolecular contacts in both forms are very similar to hydrogen-bonded zigzag
216 chains formed between the carbonylic oxygen and the aromatic protons. Moreover, the same self-

217 assembled dimers are formed through weak hydrogen bonds between the sulfoxide oxygens and ethyl
218 groups, and finally the same stacked configuration between aromatic rings are also observed. However,
219 an important packing difference is present as a consequence of a noncrystallographic inversion center in
220 one of every three layers (highlighted in Figure 9) in form II with respect to form I. Thus, forms I and II
221 can be considered morphotropic polymorphs since a noncrystallographic rearrangement transforms one
222 form into the other.⁴¹

223 In spite of the considerable research conducted with solvated drugs, the mechanisms that explain the
224 solvate formation are still unclear. However, two different mechanisms (or a combination of both) in
225 which solvent molecules incorporate into the crystal lattice have been postulated: solvent molecules can
226 provide extra intermolecular interactions (a) and/or they help to decrease voids in the crystal (b).⁴² In
227 order to assess the stability of the less dense anhydrous form II, the potential to absorb water and
228 acetonitrile of both anhydrous forms has been tested. DVS experiments have been performed, and they
229 show that form I only absorbs 0.23 and 0.73% moisture at 25 and 40 °C respectively, while form II
230 absorbs 4.64 and 1.36% moisture at 25 °C (Figure 10) and 40 °C respectively (see Supporting
231 Information for further detail). The fact that form II absorbs more water than form I when exposed to
232 high relative humidity can be due to the presence of bigger voids in form II that attract more water by
233 capillary condensation. The formation of new hydrates has not been detected by PXRD analysis of the
234 resulting samples after the DVS experiments. Moreover, a low percentage of form I was detected in the
235 sample which was initially form II, which suggests a water-assisted phase transition, as has been shown
236 for paracetamol.⁴³

237 On the other hand, when exposed to acetonitrile vapors, both anhydrous forms convert into solvate form
238 ACNII but not to solvate form ACNI, which suggests that the 1:1 acetonitrile solvate is formed through
239 a dissolution/recrystallization process, while the 2:1 acetonitrile solvate is formed by solvent diffusion.
240 Finally, a new propanenitrile solvate was discovered during the solid forms screening. Interestingly,
241 although acetonitrile and propanenitrile only differ in one methylene group, the crystal structures of both
242 solvates are dramatically different, with the structure of the propanenitrile solvate resembling that of
243 anhydrous form I (Figure 11). Desolvation under a vacuum of the propanenitrile solvate produced
244 anhydrous form I, an expected outcome due to the packing similarity between both forms.

245

246

247

248

249 **4. CONCLUSION**

250

251 In summary, we have discovered a new anhydrous form of sildenafil (form II) which is a desolvate of a
252 new 1:1 acetonitrile solvate. Both anhydrous forms are morphotropically related, and the presence of
253 voids in form II are created by desolvation of the acetonitrile solvate. Although 54 organic solvents have
254 been tested during the solid forms, screening the new polymorph is only obtained when acetonitrile is
255 used. Thus, this study highlights the importance of intensive solvate screening during early stages of a
256 polymorph/cocrystal screen of APIs because some solvates can be precursors and provide the key to the
257 discovery of potential metastable polymorphs that otherwise would remain unknown.

258

259 **AUTHOR INFORMATION**

260 **Corresponding Author**

261 *E-mail: rafel@ccit.ub.edu.

262 **ORCID**

263 Rafel Prohens: 0000-0003-0294-1720

264 **Notes**

265 The authors declare no competing financial interest.

266

267

268

269

270 **REFERENCES**

271

- 272 (1) Healy, A. M.; Worku, Z. A.; Kumar, D.; Madi, A. M. Pharmaceutical solvates, hydrates and
273 amorphous forms: A special emphasis on cocrystals. *Adv. Drug Delivery Rev.* 2017, 117,
274 25–46.
- 275 (2) Braun, D. E.; Griesser, U. J. Stoichiometric and Nonstoichiometric Hydrates of Brucine. *Cryst.*
276 *Growth Des.* 2016, 16, 6111–6121.
- 277 (3) Saleki-Gerhardt, A.; Stoweell, J. G.; Byrn, S. R.; Zografí, G. Hydration and dehydration of
278 crystalline and amorphous forms of raffinose. *J. Pharm. Sci.* 1995, 84 (3), 318–323.
- 279 (4) Braun, D. E.; Koztecki, L. H.; McMahon, J. A.; Price, S. L.; Reutzel-Edens, S. M. Navigating
280 the Waters of Unconventional Crystalline Hydrates. *Mol. Pharmaceutics* 2015, 12, 3069–3088.
- 281 (5) Rajjada, D.; Bond, A. D.; Larsen, F. H.; Cornett, C.; Qu, H.; Rantanen, J. Exploring the Solid-
282 Form Landscape of Pharmaceutical Hydrates: Transformation Pathways of the Sodium
283 Naproxen Anhydrate-Hydrate System. *Pharm. Res.* 2013, 30, 280–289.
- 284 (6) Henck, J. O.; Griesser, U. J.; Burger, A. Polymorphie von Arzneistoffen: Eine wirtschaftliche
285 Herausforderung? *Pharm. Ind.* 1997, 59, 165–169.
- 286 (7) Vippagunta, S. R.; Brittain, H. G.; Grant, D. J. Crystalline solids. *Adv. Drug Delivery Rev.*
287 2001, 48, 3–26.
- 288 (8) Byrn, S. R.; Pfeiffer, R. R.; Stowell, J. G. *Solid-State Chemistry of Drugs*, 2nd ed.; SSCI Inc.:
289 West Lafayette, Ind: 1999.
- 290 (9) Görbitz, C. H.; Hersleth, H. P. On the inclusion of solvent molecules in the crystal structures of
291 organic compounds. *Acta Crystallogr., Sect. B: Struct. Sci.* 2000, 56, 526–534.
- 292 (10) Infantes, L.; Fábíán, L.; Motherwell, W. D. S. Organic crystal hydrates: what are the important
293 factors for formation. *CrystEngComm* 2007, 9, 65–71
- 294 (11) Takiuddin, K.; Khimyak, Y. Z.; Fábíán, L. Prediction of Hydrate and Solvate Formation Using
295 Statistical Models. *Cryst. Growth Des.* 2016, 16, 70–81.
- 296 (12) Byrn, S. R.; Zografí, G.; Chen, X. *Solid-State Properties of Pharmaceutical Materials*; John
297 Wiley & Sons, 2017;.

- 298 (13) Threlfall, T. Polymorphs, Solvates and Hydrates. Handbook of Vibrational Spectroscopy; John
299 Wiley & Sons, 2006.
- 300 (14) Berziņš, A.; Skarbulis, E.; Reķis, T.; Actiņš, A. On the Formation of Droperidol Solvates:
301 Characterization of Structure and Properties. *Cryst. Growth Des.* 2014, 14, 2654–2664.
- 302 (15) Bingham, A. L.; Hughes, D. S.; Hursthouse, M. B.; Lancaster, R. W.; Tavener, S.; Threlfall, T.
303 L. Over one hundred solvates of sulfathiazole. *Chem. Commun.* 2001, 0, 603–604.
- 304 (16) Byard, S.; Abraham, A.; Boulton, P. J. T.; Harris, R. K.; Hodgkinson, P. A multi-technique
305 approach to the study of structural stability and desolvation of two unusual channel hydrate
306 solvates of finasteride. *J. Pharm. Sci.* 2012, 101, 176–186.
- 307 (17) Lee, D. C.; Webb, M. L. *Pharmaceutical Analysis*; Wiley-Blackwell, 2009.
- 308 (18) Hilfiker, R. *Polymorphism: In the Pharmaceutical Industry*; Wiley-VCH, 2006.
- 309 (19) Brittain, H. G. *Polymorphism in Pharmaceutical Solids*, 2nd ed. Informa Healthcare USA, Inc.,
310 2009.
- 311 (20) Kitaigorodskii, A. I. The Principle of Close Packing and the Condition of Thermodynamic
312 Stability of Organic Crystals. *Acta Crystallogr.* 1965, 18, 585–590.
- 313 (21) Apperley, D. C.; Markwell, A. F.; Frantsuzov, I.; Illott, A. J.; Harris, R. K.; Hodgkinson, P.
314 NMR characterisation of dynamics in solvates and desolvates of formoterol fumarate. *Phys.*
315 *Chem. Chem. Phys.* 2013, 15, 6422–6430.
- 316 (22) Stephenson, G. A.; Groleau, E. G.; Kleemann, R. L.; Xu, W.; Rigsbee, D. R. Formation of
317 isomorphic desolvates: Creating a molecular vacuum. *J. Pharm. Sci.* 1998, 87, 536–542.
- 318 (23) SADABS Bruker AXS; Madison, Wisconsin, USA, 2004. SAINT, Software Users Guide,
319 Version 6.0; Bruker Analytical X-ray Systems: Madison, WI, 1999. Sheldrick, G. M. SADABS
320 v2.03: Area-Detector Absorption Correction; University of Göttingen: Germany, 1999. SAINT,
321 Version 7.60A; Bruker AXS, 2008. SADABS, V. 2008-1, 2008.
- 322 (24) Sheldrick, G. M. A short history of SHELX. *Acta Crystallogr., Sect. A: Found. Crystallogr.*
323 2008, 64, 112–122.
- 324 (25) Boultif, A.; Louër, D. Indexing of powder diffraction patterns for low-symmetry lattices by the
325 successive dichotomy method. *J. Appl. Crystallogr.* 1991, 24, 987–993.
- 326 (26) Spartan'10; Wavefunction Inc., Irvin, CA.

- 327 (27) Favre-Nicolin, V.; Černý, R. FOX, 'free objects for crystallography': a modular approach to ab
328 initio structure determination from powder diffraction. *J. Appl. Crystallogr.* 2002, 35, 734–743.
- 329 (28) Rodriguez-Carvajal, J. Recent advances in magnetic structure determination by neutron powder
330 diffraction. *Phys. B* 1993, 192, 55–69.
- 331 (29) Stepanovs, D.; Mishnev, A. Molecular and Crystal Structure of Sildenafil Base. *Z. Naturforsch.,*
332 *B: J. Chem. Sci.* 2012, 67, 491–494 CSD code QEGTUT.
- 333 (30) Barnett, C. F.; Machado, R. F. Sildenafil in the treatment of pulmonary hypertension. *Vasc*
334 *Health Risk Manag.* 2006, 2 (4), 411–422.
- 335 (31) Galiè, N.; Hoepfer, M. M.; Humbert, M.; Torbicki, A.; Vachiery, J. L.; Barbera, J. A.; Beghetti,
336 M.; Corris, P.; Gaine, S.; Gibbs, J. S.; Gomez-Sanchez, M. A.; Jondeau, G.; Klepetko, W.;
337 Opitz, C.; Peacock, A.; Rubin, L.; Zellweger, M.; Simonneau, G. ESC Committee for Practice
338 Guidelines (CPG) Guidelines for the diagnosis and treatment of pulmonary hypertension: The
339 Task Force for the Diagnosis and Treatment of Pulmonary Hypertension of the European
340 Society of Cardiology (ESC) and the European Respiratory Society (ERS), endorsed by the
341 International Society of Heart and Lung Transplantation (ISHLT). *Eur. Heart J.* 2009, 30 (20),
342 2493–2537.
- 343 (32) Jung, S. Y.; Seo, Y. G.; Kim, G. K.; Woo, J. S.; Yong, C. S.; Choi, H. G. Comparison of the
344 solubility and pharmacokinetics of sildenafil salts. *Arch. Pharmacol Res.* 2011, 34 (3), 451–454.
- 345 (33) Methanol, ethanol, IPA, butanol, 1-propanediol, glycerol, ethylene glycol, 2-methoxyethanol,
346 1-propanol, 1-pentanol, 1-octanol, 2,2,2-trifluoroethanol, benzyl alcohol, ACN, propionitrile,
347 MEK, acetone, MiBK, water, DMF, DMSO, pentane, heptane, cyclohexane, hexane,
348 methylcyclohexane, toluene, xylene, mesitylene, anisole, 2-nitrotoluene, nitrobenzene, AcOEt,
349 isopropyl acetate, diethylether, THF, 1-methyl-2-pyrrolidone, dimethyl ethylene glycol,
350 diisopropyl ether, dioxane, iodomethane, dichloromethane, 1,2-dichloroethane, chloroform, 1,1,1-
351 trichloroethane, 1,1,2-trichloroethane, formic acid, acetic acid, trifluoroacetic acid, propanoic
352 acid, NH₃ (32%) in water, diethylamine, trimethylamine, and pyridine.
- 353 (34) Barbas, R.; Prohens, R.; Font-Bardia, M.; Bauza, A.; Frontera, A.; Prohens, R. Hydrogen
354 bonding versus π -interactions: their key competition in sildenafil solvates. *CrystEngComm*
355 2018, in press.
- 356 (35) Cruz-Cabeza, A. J.; Bernstein, J. Conformational Polymorphism. *Chem. Rev.* 2014, 114 (4),
357 2170–2191.

- 358 (36) Spackman, M. A.; Mckinnon, J. J. Fingerprinting intermolecular interactions in molecular
359 crystals. *CrystEngComm* 2002, 4, 378–392.
- 360 (37) Mckinnon, J. J.; Jayatilaka, D.; Spackman, M. A. Towards quantitative analysis of
361 intermolecular interactions with Hirshfeld surfaces. *Chem. Commun.* 2007, 0, 3814–3816.
- 362 (38) Spackman, M. A.; Jayatilaka, D. Hirshfeld surface analysis. *CrystEngComm* 2009, 11, 19–32.
- 363 (39) Rowland, R. S.; Taylor, R. Intermolecular Nonbonded Contact Distances in Organic Crystal
364 Structures: Comparison with Distances Expected from van der Waals Radii. *J. Phys. Chem.*
365 1996, 100, 7384–7391.
- 366 (40) Dunitz, J. D.; Gavezzotti, A. Attractions and Repulsions in Molecular Crystals: What Can Be
367 Learned from the Crystal Structures of Condensed Ring Aromatic Hydrocarbons? *Acc. Chem.*
368 *Res.* 1999, 32 (8), 677–684.
- 369 (41) Kalman, A. Morphotropism: link between the isostructurality, polymorphism and
370 (stereo)isomerism of organic crystals. *Acta Crystallogr., Sect. B: Struct. Sci.* 2005, 61, 536–547.
- 371 (42) Price, C. P.; Glick, G. D.; Matzger, A. J. Dissecting the Behavior of a Promiscuous Solvate
372 Former. *Angew. Chem., Int. Ed.* 2006, 45, 2062–2066.
- 373 (43) Kachrimanis, K.; Fucke, K.; Noisternig, M.; Siebenhaar, B.; Griesser, U. J. Effects of Moisture
374 and Residual Solvent on the Phase Stability of Orthorhombic Paracetamol. *Pharm. Res.* 2008,
375 25, 1440–1449.

377 **Legends to figures**

378

379 **Figure. 1.** Molecular structure of sildenafil.

380

381 **Figure. 2** Final Rietveld plot for the crystal structure refinement of sildenafil form II. Agreement
382 factors: Rwp = 12.3%, Chi2 = 4.93. The plot shows the experimental PXRD profile (red marks), the
383 calculated PXRD profile (black solid line), and the difference profile (blue, lower line). Tick marks
384 indicate peak positions.

385

386 **Figure. 3** PXRD diagrams of acetonitrile solvates form I (simulated from crystal structure) and II.

387

388 **Figure. 4** DSC thermograms of anhydrous forms I (mp onset: 189°C; enthalpy: 87.1 J/g) and II (mp
389 onset: 188 °C; enthalpy: 92.4 J/g) and solvate form ACNII (mp onset: 184 °C; enthalpy: 75.6 J/g) of
390 sildenafil.

391

392 **Figure. 5** Crystal structures of anhydrous form II and ACN solvate form ACNI.

393

394 **Figure. 6** Overlap of sildenafil molecules of anhydrous forms I (blue) and II (red). The computed
395 RMSD is 0.338 Å.

396

397 **Figure. 7** Fingerprint plots computed from Hirshfeld surfaces of form I (left) and form II (right). Strong
398 H···O contacts are highlighted in red and H···H contacts in black.

399

400 **Figure. 8** Calculated voids of anhydrous forms of sildenafil.

401

402 **Figure. 9** Packing in the b axis direction showing the layer involved in a noncrystallographic inversion
403 center.

404

405 **Figure. 10** Dynamic vapor sorption isotherms of form I (a) and form II (b) at 25 °C.

406

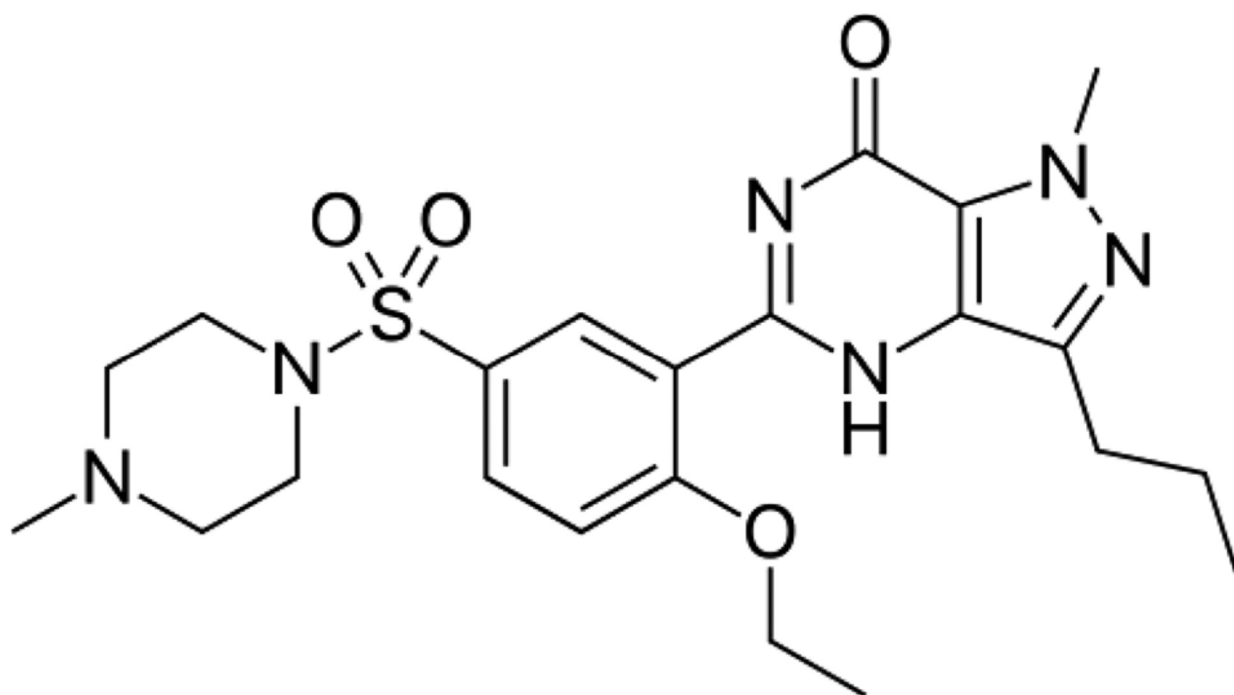
407 **Figure. 11** Crystal structures of anhydrous form I, propanenitrile solvate, anhydrous form II, and
408 acetonitrile solvate form ACNI.

409

410

411
412
413

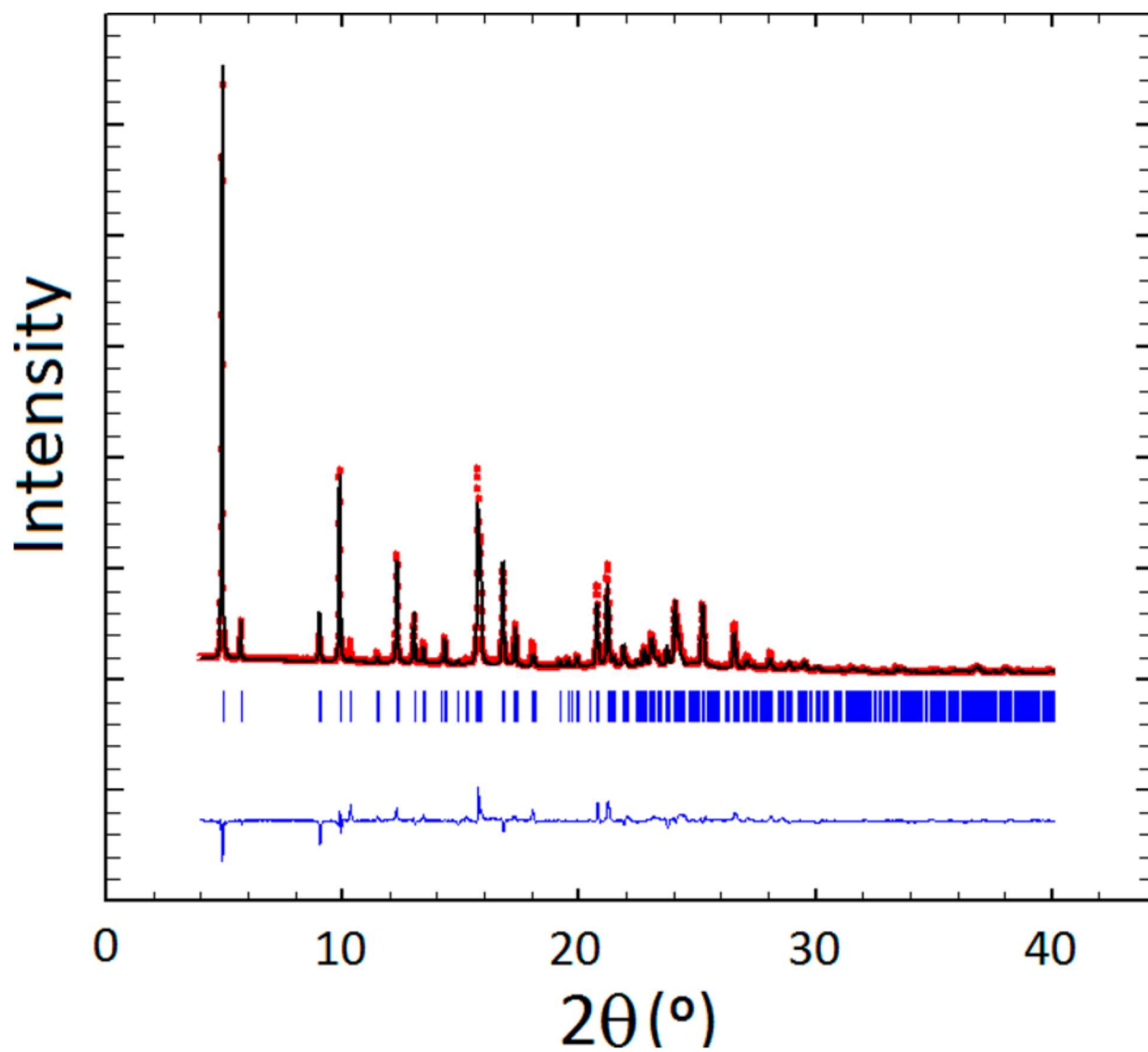
FIGURE 1



414
415
416

417
418
419

FIGURE 2



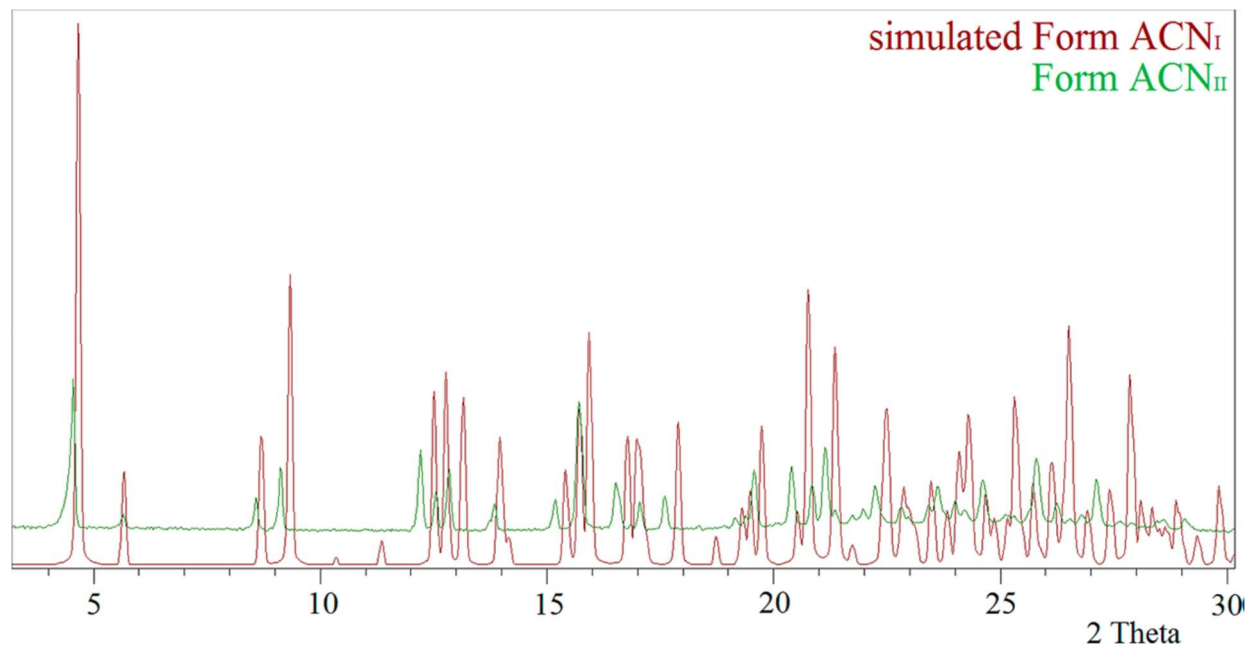
420
421

422

FIGURE 3

423

424



425

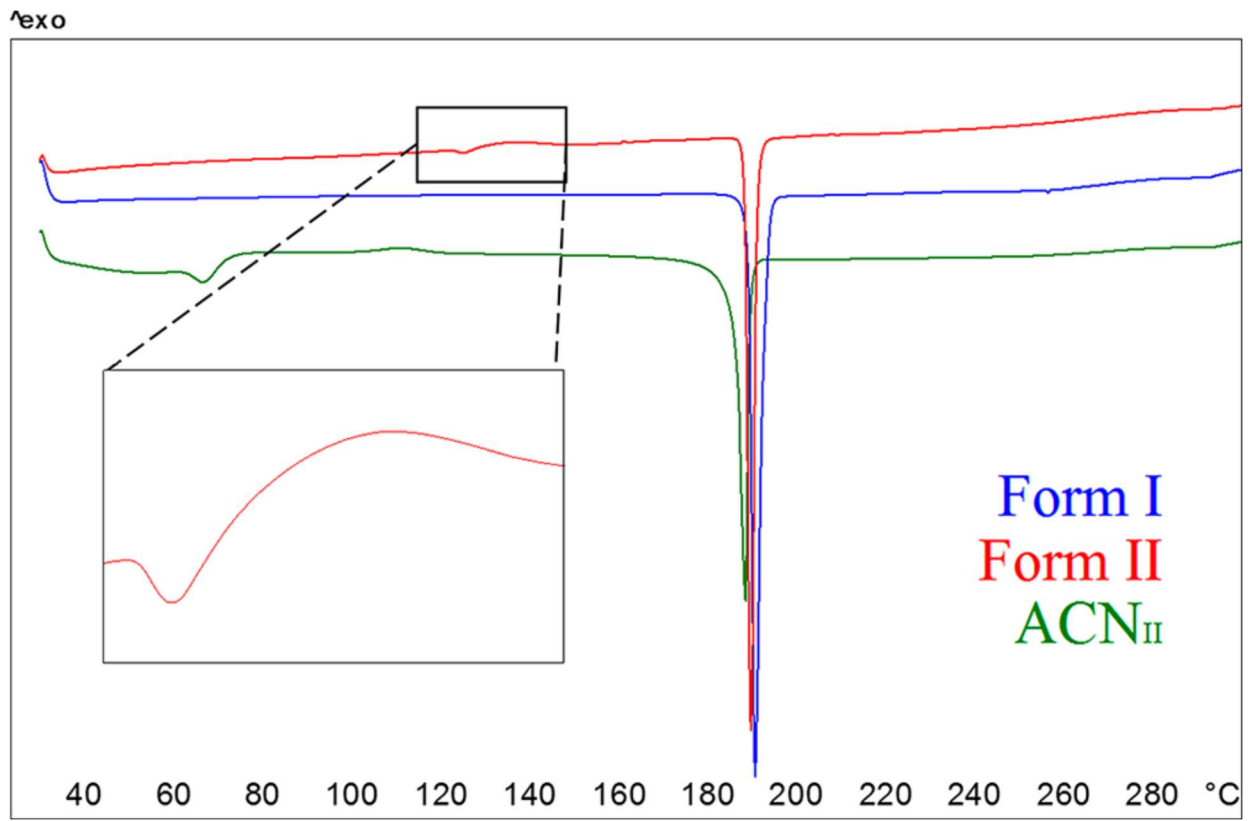
426

427

FIGURE 4

428

429



430

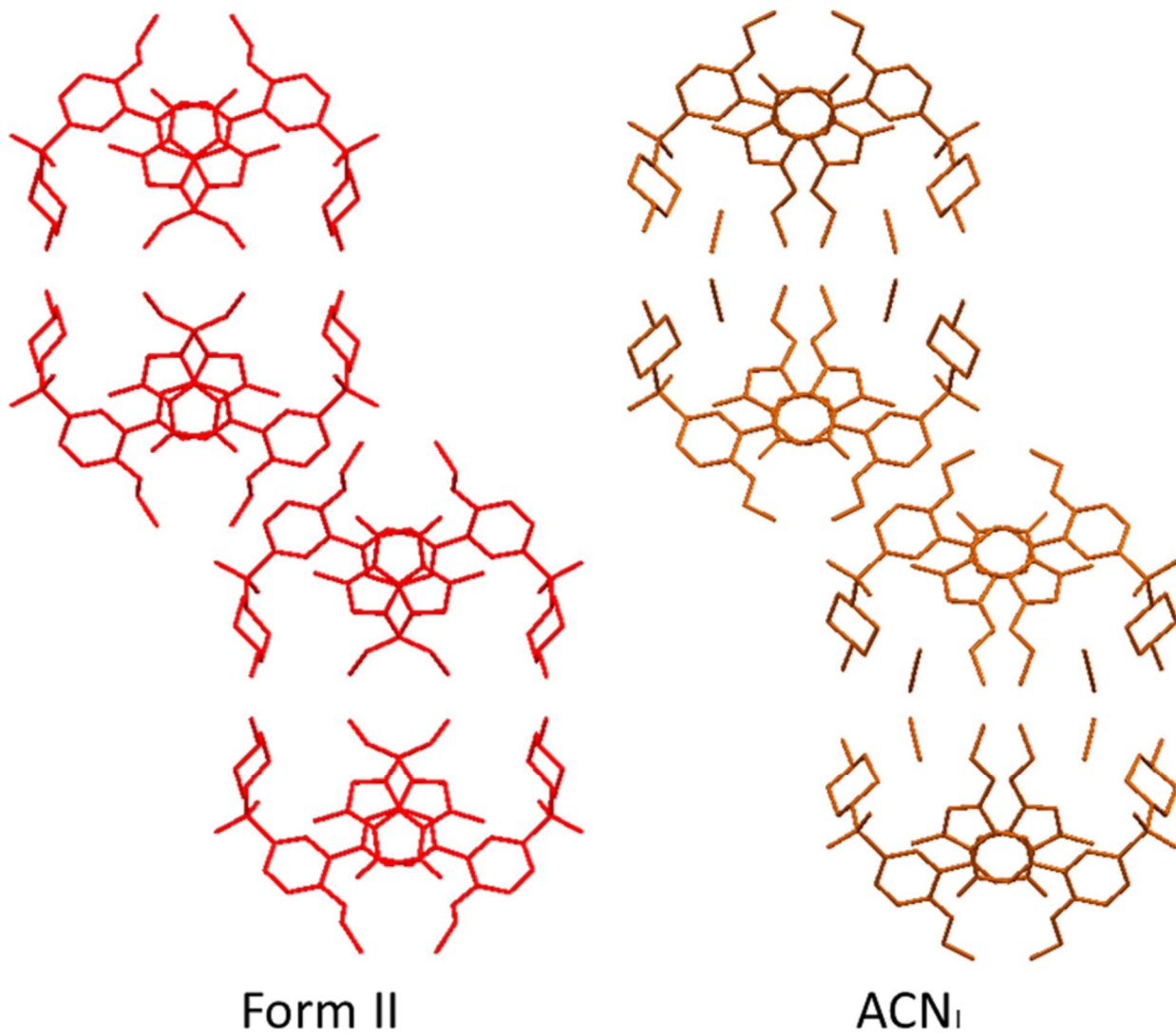
431

432

FIGURE 5.

433

434



435

436

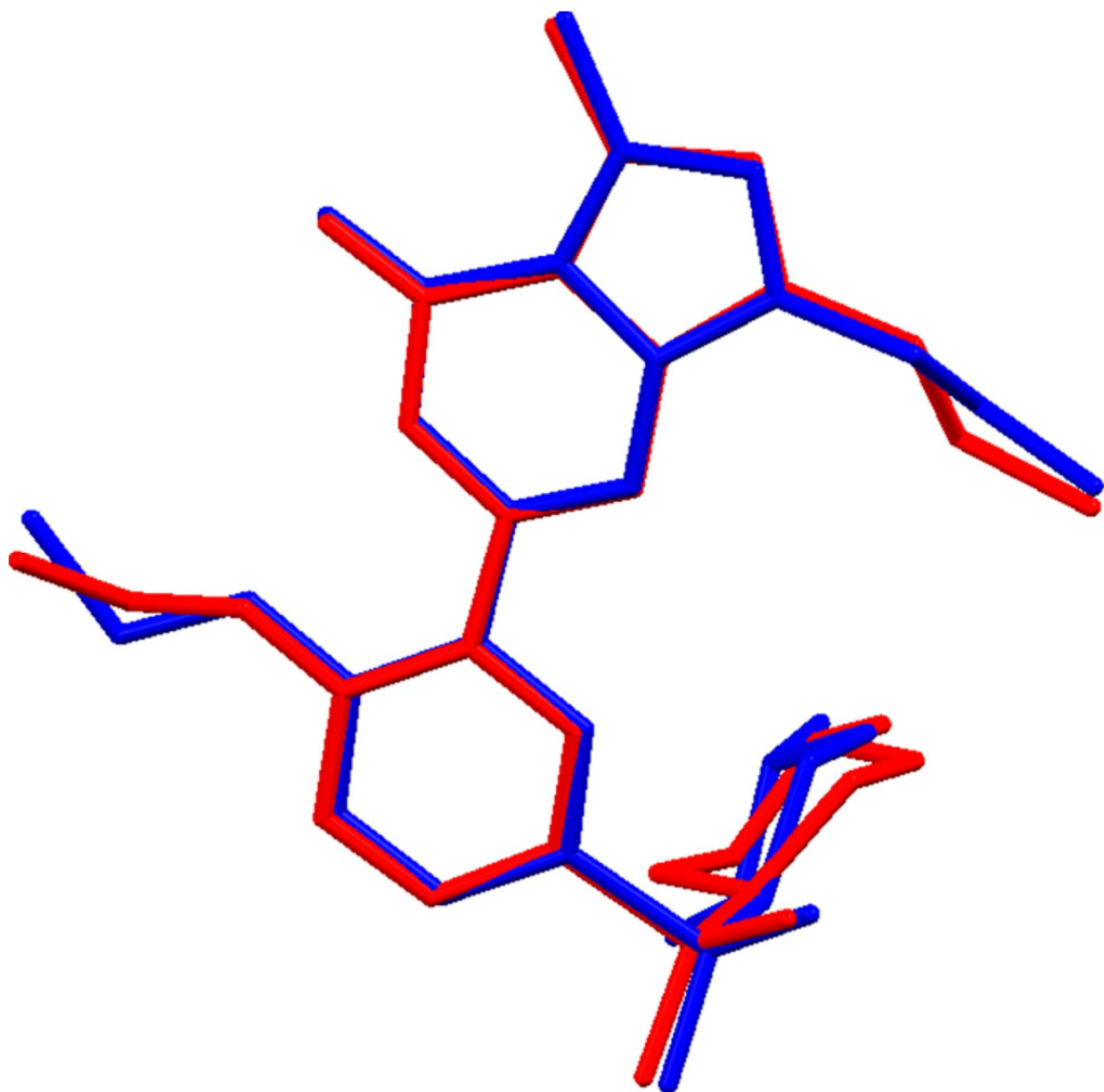
437

438

FIGURE 6.

439

440



441

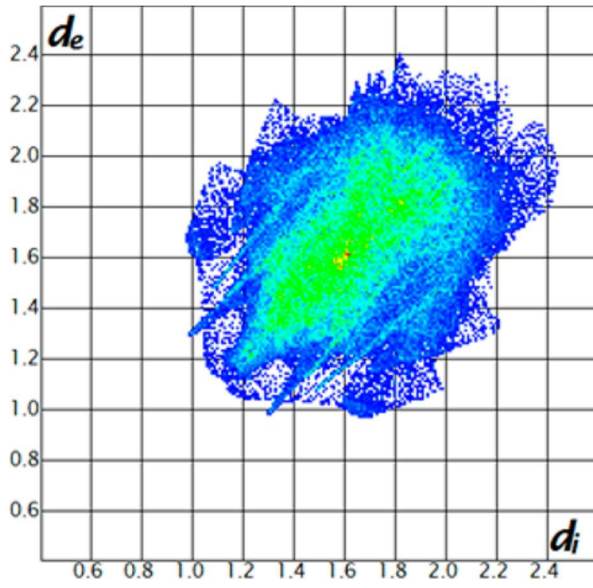
442

443

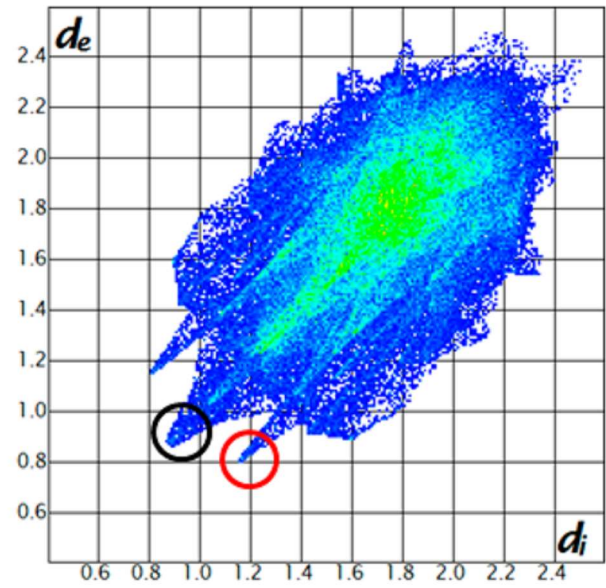
FIGURE 7.

444

445



Form I



Form II

446

447

448

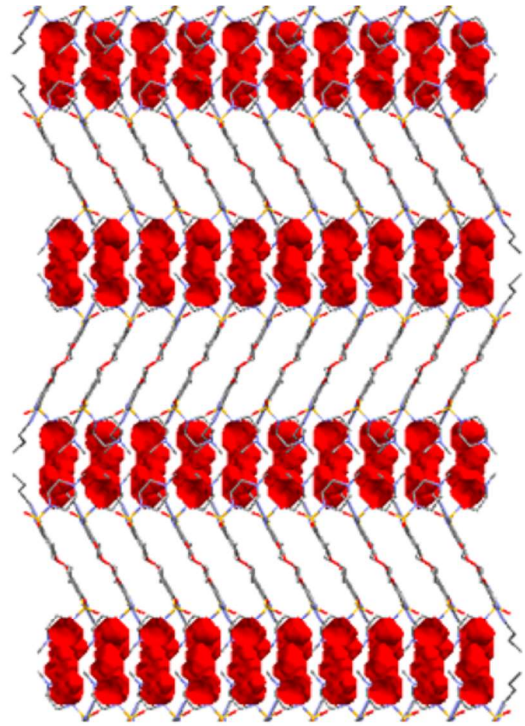
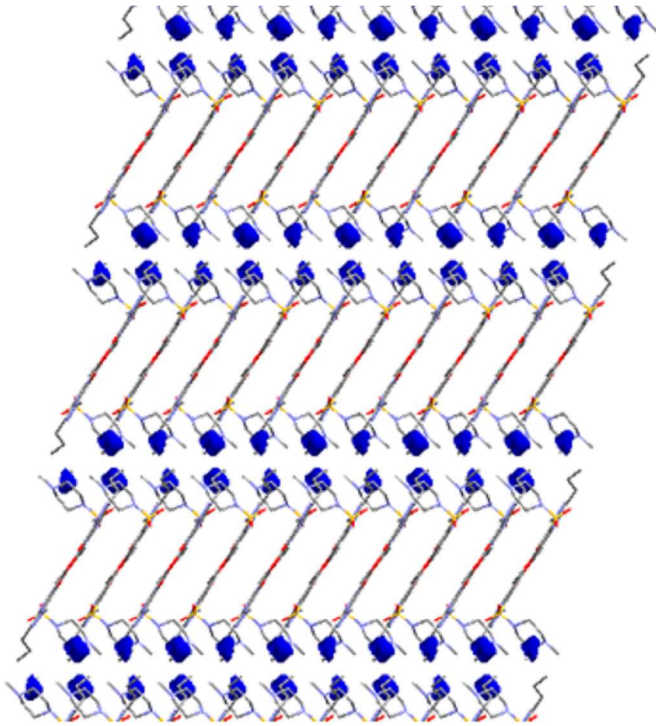
449

450

FIGURE 8.

451

452



453

Form I

Form II

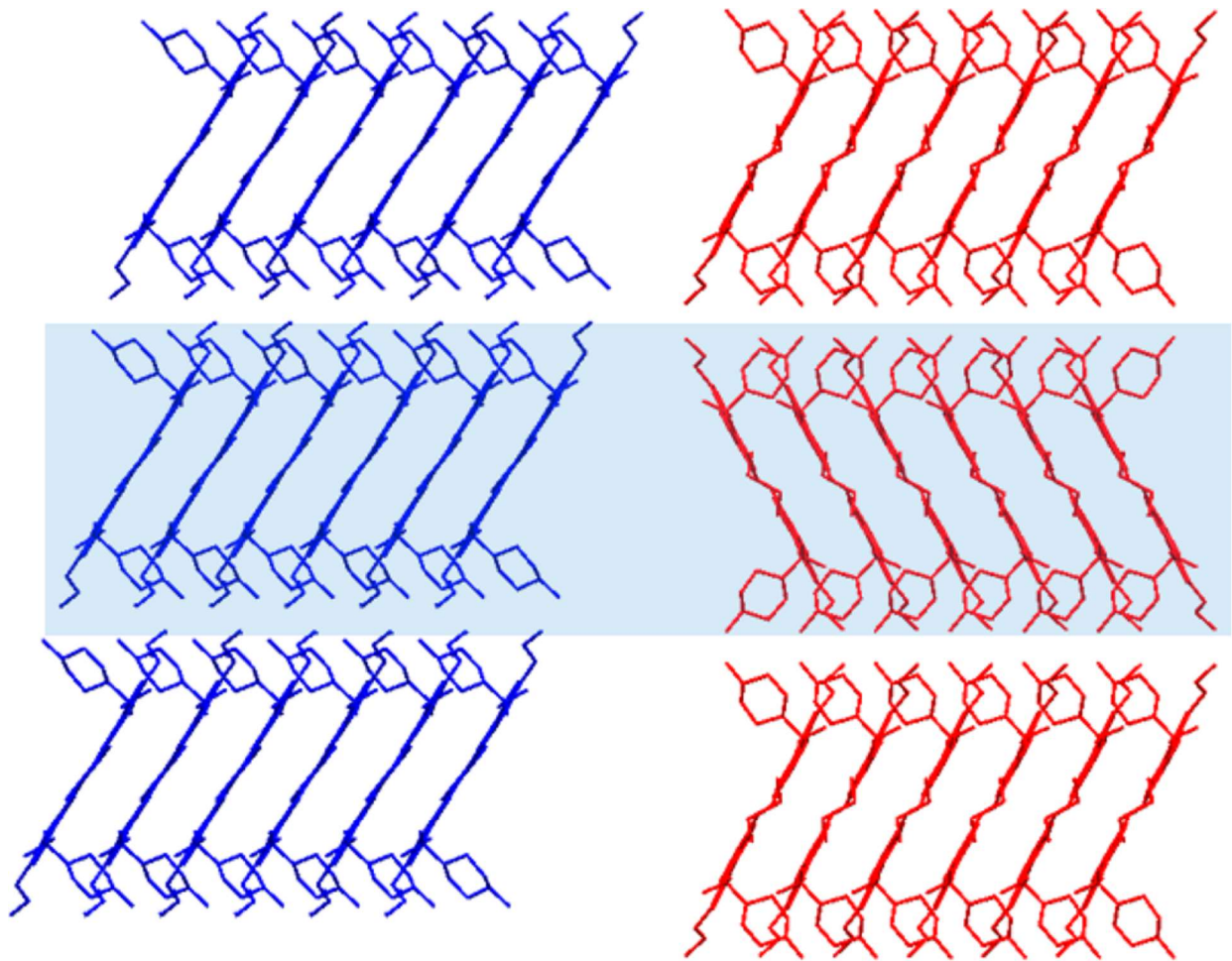
454

455

FIGURE 9.

456

457



458

Form I

Form II

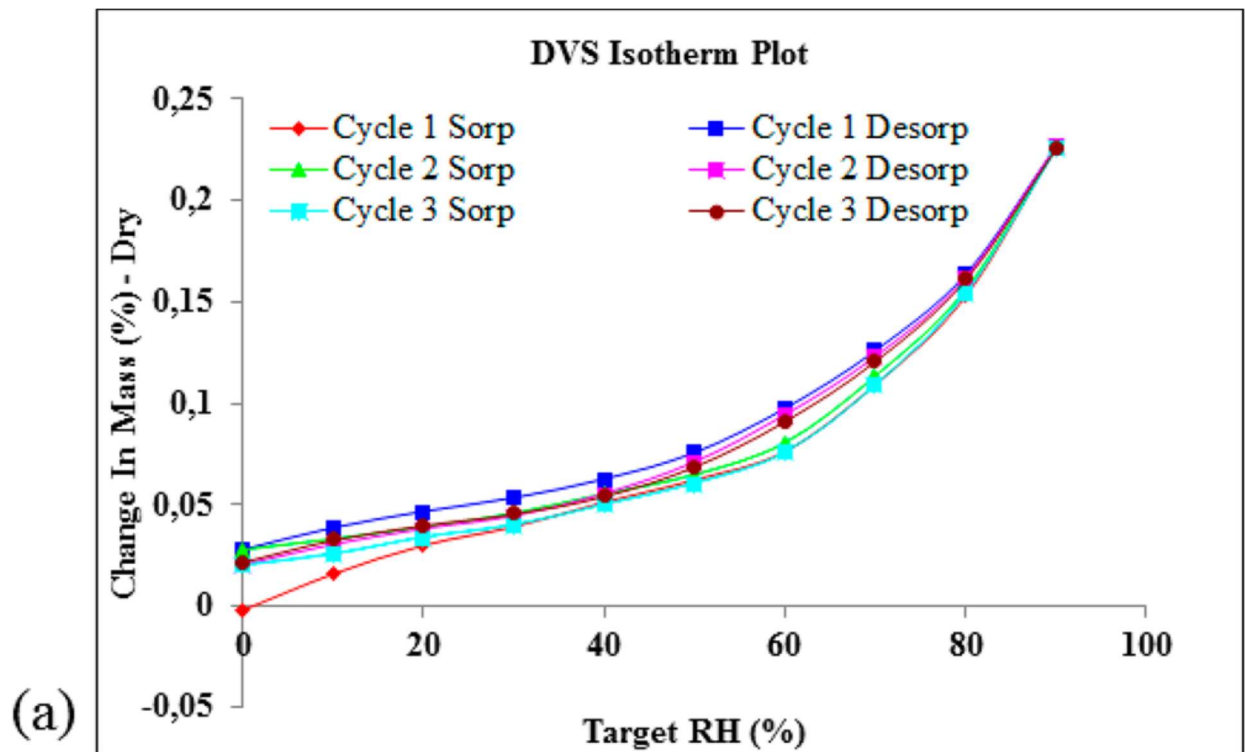
459

460

FIGURE 10.

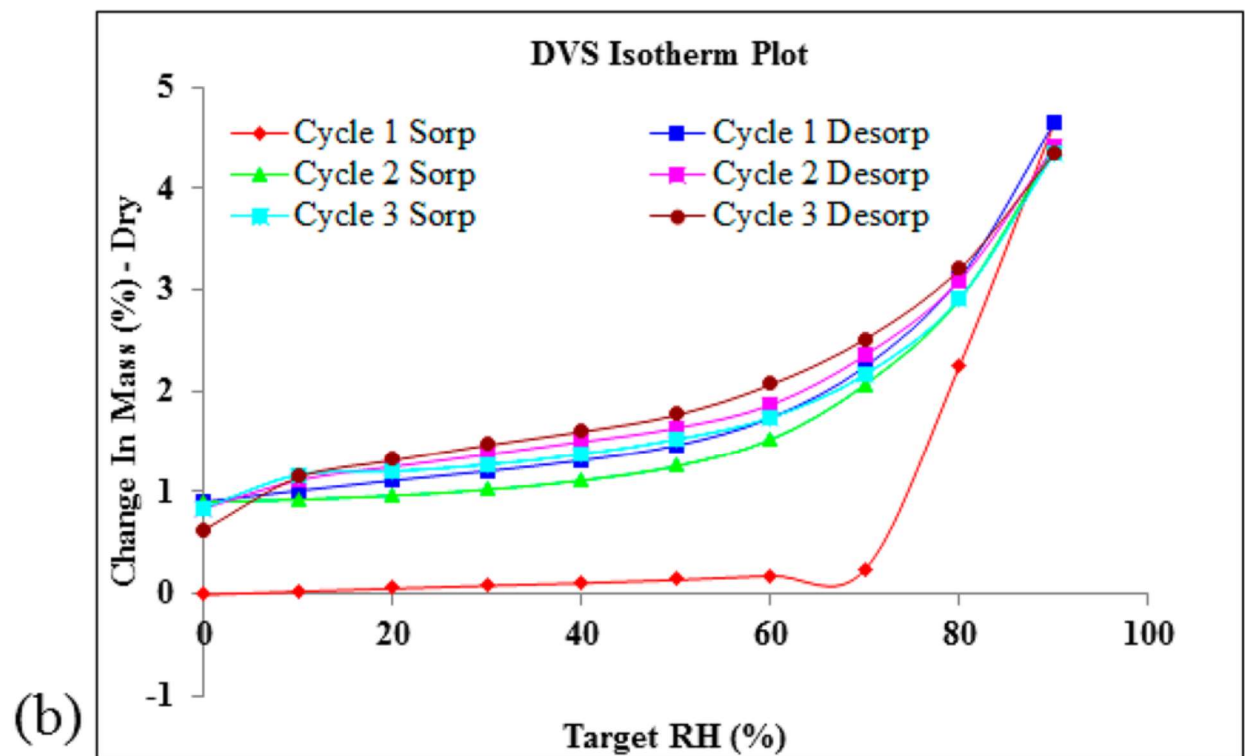
461

462



463

464

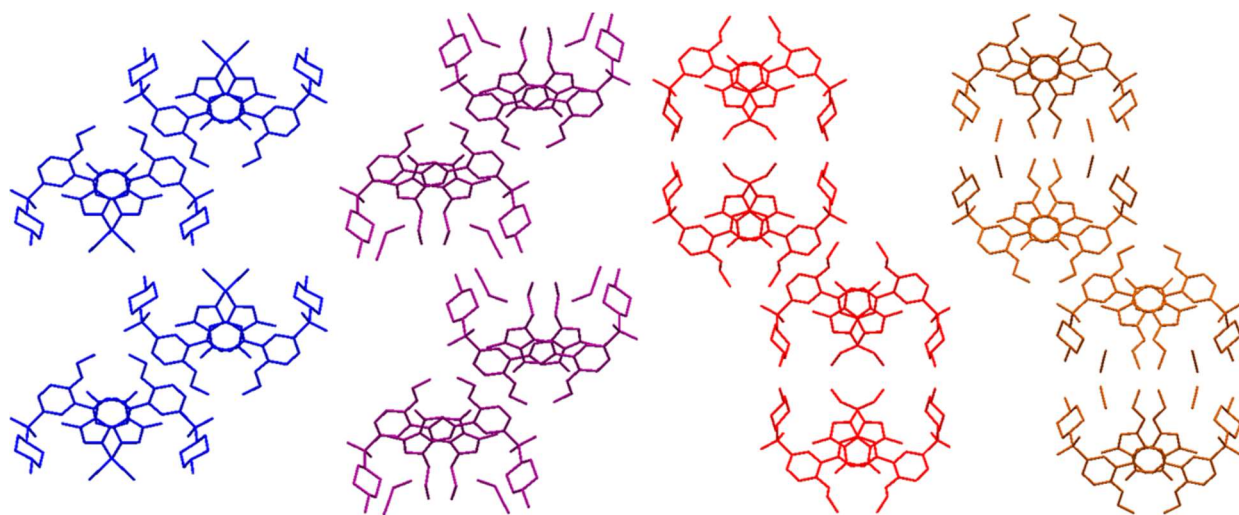


465

FIGURE 11.

466

467



468

Form I

Propanenitrile solvate

Form II

ACN_i

469

470

471 **Table 1** Crystal Data and Structure Refinement Parameters for the Different Forms of Sildenafil

472

structure	form I	form II	acetonitrile solvate form ACN ₁	propanenitrile solvate
empirical formula	C ₂₂ H ₂₆ N ₄ O ₅ S	C ₂₂ H ₂₆ N ₄ O ₅ S	C ₂₄ H ₂₈ N ₄ O ₅ S	C ₂₇ H ₃₂ N ₄ O ₅ S
molecular weight	474.58	474.58	515.63	529.66
temperature (K)	302(2)	298(2)	293(2)	100(2)
wavelength (Å)	0.71073	1.5406	0.71073	0.71073
crystal system	monoclinic	orthorhombic	orthorhombic	monoclinic
space group	P21/c	Pca	Pca	P21/c
a, b, c (Å)	17.301(4) 17.072(3) 8.3324(17)	35.713(1) 17.0949(4) 8.1146(1)	17.0918(16) 37.876(4) 7.9351(7)	19.3079(9) 14.8253(6) 9.2680(4)
α, β, γ (deg)	90 99.222(8) 90	90 90 90	90 90 90	90 90.720(2) 90
volume (Å ³)	2429.3(9)	4954.0(2)	5136.9(9)	2652.7(2)
Z, density (calc) (Mg/m ³)	4, 1.298	8, 1.273	8, 1.333	4, 1.326
absorption coefficient (mm ⁻¹)	0.173		0.171	0.167
F(000)	1008		2192	1128
crystal size (mm ³)	0.275 × 0.140 × 0.108		0.236 × 0.148 × 0.066	0.222 × 0.124 × 0.073
θ range for data collection (deg)	2.386 to 26.345	2.0 to 80 step 0.026 (2θ)	2.383 to 26.435	2.518 to 26.452
limiting indices	-21 ≤ h ≤ 21 -21 ≤ k ≤ 21 -10 ≤ l ≤ 10		-18 ≤ h ≤ 21 -38 ≤ k ≤ 47 -9 ≤ l ≤ 9	-24 ≤ h ≤ 24 -18 ≤ k ≤ 18 -11 ≤ l ≤ 11
reflections collected/unique	39306/4943 [R(int) = 0.1201]		26368/5240 [R(int) = 0.1755]	50725/5407 [R(int) = 0.0555]
completeness to θ = 25.242° (%)	99.9		99.8	99.0
absorption correction	semiempirical from equivalents		semiempirical from equivalents	semiempirical from equivalents
max and min transmission	0.7454 and 0.6855		0.7454 and 0.5871	0.7454 and 0.6943
refinement method	full-matrix least-squares on F ²	Rietveld	full-matrix least-squares on F ²	full-matrix least-squares on F ²
data/restraints/parameters	4943/0/310	3712/66/10	5240/0/346	5407/0/342
goodness-of-fit on F ²	1.016		0.999	1.035
final R indices [I > 2σ(I)]	R ₁ = 0.0543, wR ₂ = 0.1075	R _{wp} = 12.3	R ₁ = 0.0838, wR ₂ = 0.1638	R ₁ = 0.0446, wR ₂ = 0.1040
R indices (all data)	R ₁ = 0.1327, wR ₂ = 0.1336	Chi2 = 4.93	R ₁ = 0.2017, wR ₂ = 0.2077	R ₁ = 0.0603, wR ₂ = 0.1128
largest diff. peak and hole (e Å ⁻³)	0.176 and -0.295		0.383 and -0.328	1.59 and -0.702
CCDC	1821370	1832582	1821373	1821372

473